

When does TMAO fold a polymer chain and urea unfold it?

Jagannath Mondal, Guillaume Stirnemann, and B. J. Berne*
Department of Chemistry, Columbia University, New York, NY 10027
(Dated: October 8, 2018)

Longstanding mechanistic questions about the role of protecting osmolyte trimethylamine *N*-oxide (TMAO) which favors protein folding and the denaturing osmolyte urea are addressed by studying their effects on the folding of uncharged polymer chains. Using atomistic molecular dynamics simulations, we show that 1-M TMAO and 7-M urea solutions act dramatically differently on these model polymer chains. Their behaviors are sensitive to the strength of the attractive dispersion interactions of the chain with its environment: when these dispersion interactions are high enough, TMAO suppresses the formation of extended conformations of the hydrophobic polymer as compared to water, while urea promotes formation of extended conformations. Similar trends are observed experimentally on real protein systems. Quite surprisingly, we find that *both* protecting and denaturing osmolytes strongly interact with the polymer, seemingly in contrast with existing explanations of the osmolyte effect on proteins. We show that what really matters for a protective osmolyte is its effective depletion as the polymer conformation changes, which leads to a negative change in the preferential binding coefficient. For TMAO, there is a much more favorable free energy of insertion of a single osmolyte near collapsed conformations of the polymer than near extended conformations. By contrast, urea is preferentially stabilized next to the extended conformation and thus has a denaturing effect.

I. INTRODUCTION

Osmolytes are small cosolutes found endogenously to protect cells against osmotic stress¹. However, they can have profound effects on protein stability²⁻⁸. While some of them are denaturants (e.g. urea), others like trimethylamine *N*-oxide (TMAO) act as protecting osmolytes in vivo: in denaturing conditions, they bias the protein structure toward the folded conformation^{1,9-11}. They are thus referred to as chemical chaperones. Hence, TMAO is used by deep-sea organisms to counteract the deleterious effect of pressure and by sharks or skates to compensate for their relatively high concentrations of the denaturing urea. Most interestingly, the protein folding propensity of TMAO has been used experimentally to study the mechanisms involved in protein misfolding diseases, including e.g. prion protein^{12,13}, tau protein^{14,15} (Alzheimer disease) and alpha-synuclein¹⁶ (involved in numerous neurodegenerative diseases); chemical chaperones like TMAO even appear promising as therapeutics¹⁷, even though it was recently found to be related to an increased risk of car-

diovascular diseases in humans¹⁸. TMAO is active in endogenous systems for concentrations as low as 200 mM^{1,12}. Experiments in vitro on alpha-synuclein, an intrinsically disordered protein, have given evidence that this protective effect increases with concentration.¹⁶

TMAO is a small amphiphile (chemical formula: $(\text{CH}_3)_3\text{NO}$) consisting of a small hydrophilic group (N^+O^-) and a bulky hydrophobic part (3 methyl groups). Several mechanisms have been invoked to explain the folding propensity of TMAO. In a first scenario, TMAO would enhance water structure and hydrogen-bond (HB) strength, which would indirectly affect the equilibrium between the folded and the unfolded conformations of a protein.¹⁹⁻²¹ However, this mechanism has been challenged by several studies, mainly based on molecular dynamics (MD) simulations, where no significant alteration of water structure was found in aqueous solutions of TMAO²²⁻²⁴. These results may not be surprising since TMAO can only accept 2 to 3 strong HBs at its hydrophilic head, which represents less than 10% of its hydration water HB population²⁵.

Other studies have suggested that direct in-

teractions, or especially the lack thereof, between TMAO and the protein backbone could cause the osmolyte effect. In particular, thermodynamic measurements have highlighted the importance of the interactions between TMAO and the protein backbone and side-chains^{9,10}. TMAO has favorable interactions with some protein side-chains, especially the positively charged groups that can interact with the O⁻ of TMAO. In contrast, interactions with the protein backbone, in particular with the amide NH, are entropically unfavorable.²³ If these unfavorable interactions were to dominate, TMAO would be depleted from the protein surface. It has been suggested that the resulting concentration gradient in the TMAO could lead to an osmotic pressure favoring the folded conformation with respect to the unfolded one.²³ Recently, Garcia and co-workers have combined²⁶ computer simulation with the experimental osmotic pressure measurements and have suggested a mechanism where there is preferential exclusion of TMAO from protein surfaces due to repulsive self-interaction in the solvation shell. Others have argued that osmotic pressure itself cannot explain this phenomenon, and that “water mediated interactions” between the osmolyte and the protein could also play a role.²⁴

However, a clear unifying scenario has not yet emerged from the study of the effect of TMAO on proteins. One of the reasons might be the presence of amino acids with different chemical properties which might complicate the role of TMAO as a structure enhancer. Thus instead of struggling with different amino acids, a successful strategy can be to use a simple polymeric chain whose hydrophobicity can be tuned. There have already been studies of the action of TMAO on purely hydrophobic chains²², but even for such a simple system a consensus has not yet been achieved. A good illustration of the lack of consensus is the opposite conclusions reached in two different investigations. Based on simulations of a small hydrophobic solutes and of hydrophobic chains, one of these studies suggested that TMAO has a negligible effect on the hydrophobic interactions.²² In contrast other studies suggest that TMAO destroys hy-

drophobic interactions²⁷.

To investigate the molecular mechanism of TMAO’s role as a protective osmolyte, it is interesting to compare it with the effect of urea (chemical formula: $(\text{NH}_2)_2\text{CO}$) solutions that lead to the opposite behavior — unfolding of the protein. For example Pettitt and co-workers²⁸ have recently explored the conformational preferences of decaalanine in TMAO and urea solutions using free energy perturbation techniques. Their analysis, based on the decomposition of the transfer free energy, suggests the differences in the behavior of peptide in the two different solutions arises mainly from differences in the relative importances of van der Waals and electrostatic interactions: urea denaturation is dominated by van der Waals attractions whereas TMAO exerts its effect by causing unfavorable electrostatic interactions. In this contribution we extend our previous work on urea²⁹ by using similar systems and methodologies and apply it to contrast the respective role of a denaturing osmolyte (urea) and a protective osmolyte (TMAO) on uncharged chains in water. We focus on the mechanisms by which these two osmolytes produce opposite actions on the conformations of this Lennard-Jones chain. Following most of the previous simulation studies, we used concentrations higher than that found *in vivo* to enhance the osmolyte influence on protein stability. Hence we chose a concentration of 7 M for urea (consistent with Ref.²⁹) and a concentration of 1 M for TMAO. Both concentrations are widely used to study the effects of the respective osmolytes *in vitro* and *in silico*. Our study shows that while acting on the same chain, TMAO stabilizes the collapsed conformations of the chain while urea destabilizes the collapsed conformations, and the simulations later allow us to offer a molecular explanation to these different behaviors. The paper is organized as follows: the simulation model and methods are described in section II, results are presented in section III, and some conclusions are presented in section IV.

II. SIMULATION MODEL AND METHODS

System and forcefields Our system consists of a 32-bead polymer solvated in various aqueous solutions. The polymer is uncharged and the beads only interact with their environment via Lennard-Jones (LJ) potentials. While the bead radius is fixed ($\sigma_b=0.4$ nm) the hydrophobic character of the chain can be tuned by varying the energy parameter ϵ_b . Following a previous study,²⁹ four values were employed ($\epsilon_b = 0.4, 0.6, 0.8, 1.0$ kJ/mol) even if most of the current work was performed on the $\epsilon_b = 1.0$ kJ/mol polymer. Along the chain, 1-4 interactions were removed; parameters for the 1-2 (bonds) and 1-3 (angles) interactions can be found elsewhere.²⁹ For water molecules, we used the SPC/E model³⁰, while urea interacts through the OPLS/AA forcefield³¹ and TMAO through the forcefield developed by Kast et al's³². The geometric combining rules were used in the cross interactions for ϵ and arithmetic combination rules were used for σ . Three systems were simulated. The system of pure aqueous solution was composed of the polymer solvated by 4092 water molecules. The system of 1 M TMAO solution was composed of the 32-bead polymeric chain, 79 TMAO molecules and 4013 water molecules. On the other hand, the system of 7 M urea solution was composed of the 32-bead polymeric chain, 500 urea molecules and 2727 water molecules. The box size was close to $5 \times 5 \times 5$ nm³ in all cases. We have also repeated our simulation for TMAO at $\epsilon_b = 1.0$ kJ/mol using a different forcefield (called herein the "osmotic model") recently proposed by Garcia and coworkers²⁶ and we found it to follow the same qualitative trends (*c.f.* the Appendix).

Equilibrium simulations All simulations were performed using Gromacs 4.5.4 software³³. In a bid to sample different polymer conformations in different osmolyte solutions, unrestrained equilibrium MD simulations of the polymer chain were performed in pure water, 1 M TMAO and 7 M urea solutions. In order to avoid any bias, an extended configuration of the polymeric

chain was used as an initial configuration in pure water and in the aqueous solution of 1 M TMAO while a collapsed configuration of the polymer was used as an initial configuration for the simulation in aqueous solution of 7 M urea. The initial extended configuration was an all-trans configuration of the polymer while the collapsed configuration was picked from the simulation of the polymer in water. Each of the systems was first energy-minimized using a steepest-descent algorithm and then subjected to 100 ns of production run in NPT ensemble. The Nose-Hoover thermostat was used for maintaining the average temperature at 300 K and the Parinello-Rahman barostat was used for maintaining the average pressure at 1 bar. For all three aqueous solutions, unrestrained simulations were repeated for the four values of the LJ energy parameter (ϵ_b) for the polymer beads.

Potentials of mean-force We determined the free energy landscape (or potential of mean force [PMF]) of the 32-bead LJ chains along one or several collective reaction coordinates in different solutions by performing umbrella sampling simulations. We chose as reaction coordinate the polymer radius of gyration R_g in pure water, 1 M TMAO and 7 M urea. We employed the PLUMED extension of Gromacs³⁴. The value of R_g ranged from 0.4 nm to 1.2 nm at a spacing of 0.05 nm between adjacent windows. Restraining harmonic force constants of 7000 kJ/mol/nm² were used in the umbrella potential in all positions to ensure a Gaussian distribution of the reaction coordinate around each desired value of the reaction coordinate. Finally, we used the Weighted Histogram Analysis Method (WHAM).^{35,36} to generate unbiased histograms and corresponding free energies. As described later we also compute the joint probability distribution of R_g and the end-to-end distance and the corresponding potential of mean force as a function of these two variables.

Preferential interaction We employed two parameters to measure the affinity of the cosolvent (urea or TMAO) for the polymer. First, the local-bulk partition coefficient K_p was cal-

culated, where as⁷

$$K_p = \frac{\langle n_s \rangle}{\langle n_w \rangle} \cdot \frac{N_w^{tot}}{N_s^{tot}}. \quad (1)$$

Here $\langle n_X \rangle$ is the average number of molecules of type X bound to polymer and N_X^{tot} is the total number of molecules of type X in the system (where $X = s$ stands for the cosolvent (urea or TMAO) and $X = w$ stands for water). K_p is intensive and reflects the affinity of the cosolvent for the polymer regardless of the exposed surface area of the polymer. The other parameter is the experimentally-relevant preferential binding coefficient,^{2,3,7,26,37}

$$\Gamma = \left\langle n_s - \frac{N_s^{tot} - n_s}{N_w^{tot} - n_w} \cdot n_w \right\rangle, \quad (2)$$

which is extensive (i.e., it depends on the size of the hydration shell). To determine the dependence on the proximal cut-off distance for the counting of molecules around the polymer, we computed the value of both quantities K_p and Γ as a function of distance from the polymer (i.e., by examining the explicit distance dependence of $n_s(r)$ and $n_w(r)$), which is defined as the shortest distance between the central atom of the solvent molecule (O for water, N for TMAO and C for urea) and any polymer bead. Additional simulations were performed as follows. We froze 5 representative configurations of the the polymer either in the collapsed or the extended state for each osmolyte solution, and then propagated each of these simulations for 15 ns (total simulation length of 75 ns for each polymer configuration). In each case, both K_p and Γ were averaged over this ensemble of trajectories, and standard deviations were obtained via block averaging.

Finally, we used the Free Energy Perturbation (FEP) technique to compute the transfer free-energy (chemical potential) for inserting a *single* TMAO (or urea or water molecule) from bulk solution into the first solvation shell of particular conformations of polymer in 1 M TMAO (or 7 M urea) where the polymer conformation was fixed in either a collapsed or an extended conformation. For these calculations the ini-

tial configurations were taken from a representative snapshot of the prior umbrella sampling windows and the TMAO (or urea or water) molecule was grown in presence of other TMAO (or urea or water) molecules in solution. The interactions of the molecule being inserted were slowly turned on in two stages: in the first stage only the van der Waals interactions were turned on, and in the second stage the electrostatic interactions were turned on. Thermodynamic integration gives these two contributions to the transfer free energy. The difference between the free energy for the insertion proximate to the polymer and the insertion in bulk gives the required transfer free energies. Finally, since the choice of the position near the polymer where the osmolyte and solvent molecules is grown is arbitrary, we repeated such calculations at several positions in each case: 5 sites for TMAO and urea and 3 sites for water near each of collapsed and extended conformations and 2 sites of each of them in bulk media. They were finally averaged and the standard deviations were estimated.

III. RESULTS AND DISCUSSION

A. Osmolyte effect on folding equilibria

We first verify that the effects of TMAO and urea on an uncharged Lennard-Jones polymer chain are those observed in protein systems, i.e. that they act respectively as protective and denaturing osmolytes. Towards this end, a reasonable approach is to follow the time-evolution of an order parameter describing the polymer conformation, like its radius of gyration which will allow us to distinguish between the collapsed and extended configurations. Such profiles are shown for a polymer with a bead interaction parameter $\epsilon_b = 1.0$ kJ/mol in Figure 1. For these unrestrained simulations, the initial configurations in each system (water, 1 M TMAO and 7 M urea) were chosen anticipating the effect of this aqueous solution on the polymer conformational equilibrium. Thus, simulations were started from an unfolded, state in water and

TMAO solutions ($R_g = 11.5 \text{ \AA}$), and started from a collapsed configuration ($R_g = 4.5 \text{ \AA}$) in the urea solution. Each of these simulations were then propagated for 100 ns.

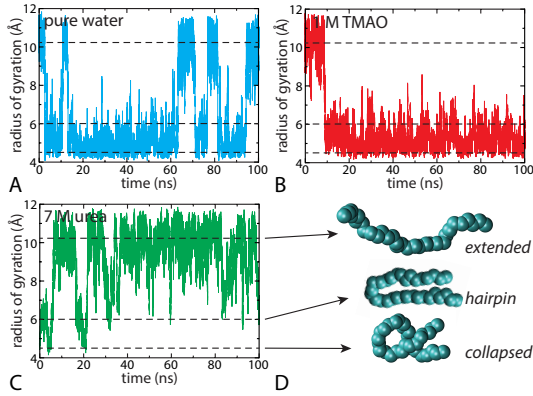


FIG. 1. Time profile of polymer’s radius of gyration for $\epsilon_b = 1.0 \text{ kJ/mol}$ as obtained from unrestrained simulations in different aqueous solutions: (A) in water, (B) in 1 M TMAO solution and (C) in 7 M urea solution. The horizontal dashed lines corresponding to $R_g = 4.5, 6.0$ and 10.2 \AA represent the most probable values of the radius of gyration for the collapsed (folded), hairpin-like and extended (unfolded) conformations respectively, depicted in (D).

Figure 1 shows that the polymeric chain behaves very differently in the three environments. In water (Figure 1A), the initially-extended polymer quickly collapses and then fluctuates between the collapsed and the extended configurations. In the TMAO solution (Figure 1B), the polymer collapses and remains compact for the whole 100-ns timescale: the extended configuration sampled in pure water is not observed in TMAO on the time scale of the simulation. In contrast, the polymer in urea unfolds, (Figure 1C) but very occasionally revisits more compact states like the hairpin at $R_g \approx 0.6 \text{ nm}$, and very rarely visits the most compact states seen in water.

We thus see that for $\epsilon_b=1.0 \text{ kJ/mol}$, TMAO and urea act respectively as protective and a denaturing osmolytes with respect to the hy-

drophobic chain. This was already observed for urea²⁹ albeit for a different water model (TIP4P³⁸). It is remarkable that these osmolytes have similar effects on the hydrophobic chain as they do on real proteins. In the following, we aim to better understand this interesting behavior.

The semi-compact hairpin configuration of the chain ($R_g \approx 0.6 \text{ nm}$) observed in the urea solution²⁹ (see Figure 1C) and to some extent in water and TMAO solution (Figure 1A and Figure 1B) can be better understood by considering a two dimensional collective coordinate consisting of the radius of gyration and the end-to-end distance of the chain. Figure 2 shows the joint probability $P(L, R_g)$ of finding a polymer ($\epsilon_b=1.0 \text{ kJ/mol}$) with end-to-end distance L and radius of gyration R_g , for each of the systems shown in in Figure 1. To avoid possible biases due to limited sampling in unperturbed simulations, the probability distribution of R_g is first recovered from the PMF obtained via umbrella-sampling simulations. In each window, we later estimate the conditional probability $P(L|R_g)$ of finding L given R_g . The joint probability is finally recovered using the relation

$$P(L, R_g) = P(L|R_g)P(R_g). \quad (3)$$

The distributions shown in Figure 2 confirm our previous findings: in urea the extended configurations are significantly more populated than in water whereas in TMAO they are essentially absent. Moreover, the hairpin state observed at $R_g \approx 0.6 \text{ nm}$ and small L in the 2D plots, although more prominent in urea solution, also appear in TMAO solution and in pure water. In contrast, the collapsed state around $R_g \approx 0.45 \text{ nm}$ corresponds to higher L , showing that in the two order parameters are largely decoupled in this region of the distribution. Unfolded configurations correspond to high values of both L and R_g and give rise to distributions elongated along the diagonal in the 2D plots and only urea has a strong peak there.

The potentials of mean force $W(R_g)$ as a function of the polymer radius of gyration R_g , obtained via umbrella sampling, corresponding probability distributions $\exp[-\beta W(R_g)]$ (for

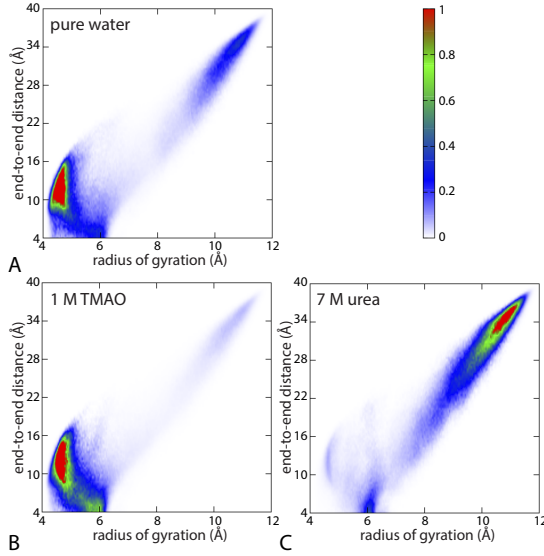


FIG. 2. Comparison of joint-probability distribution of polymer chain (with $\epsilon_b = 1$ kJ/mol) along radius of gyration and end-to-end distance (A) in water, (B) in 1 M TMAO and (C) in 7 M urea, obtained from umbrella sampling simulations.

$\epsilon_b=1.0$ kJ/mol) and for the three aqueous solutions are shown in Figure 3A and B respectively (and in the Figure 6 for other values of ϵ_b). These correspond to the projections of the joint-probability distribution onto the radius of gyration axis. These provide a more reliable and quantitative description of the polymer conformational equilibrium than simulations based on unrestrained MD trajectories (Figure 1) because those would require much longer runs (as later illustrated by the free-energy barriers of 2 to 4 kcal/mol between states).

As can be seen in Figure 3, the unfolded state in TMAO solution gets destabilized with respect to pure water, whereas the collapsed state is not dramatically affected. Quite remarkably, the unfolded state is almost totally suppressed for TMAO and its collapsed state is more compact for this case of $\epsilon_b = 1.0$ kJ/mol.

In previous molecular dynamics simulations of a similar system,²² it was found that that TMAO has little affect on the conformational

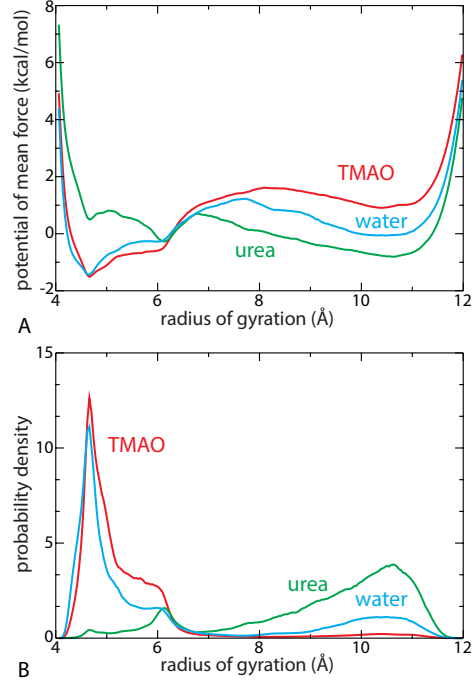


FIG. 3. Potential of mean force along the radius of gyration (A) and the corresponding probability distributions (B) in the three aqueous solutions (water, blue; TMAO, red and urea, green) for polymer chains with $\epsilon_b = 1.0$ kJ/mol. The PMFs $W(R_g)$ are normalized so that $\int_0^\infty \exp(-W(r)/k_B T) dr = 1$.

equilibrium of a hydrophobic polymer chain. In that study a lower polymer bead parameter of $\epsilon_b = 0.6$ kJ/mol was used than in our simulations. It is therefore of importance to determine the effect of smaller ϵ_b on the behavior of TMAO, as was done earlier for urea solutions²⁹. In the Appendix and Figure 6 that as the hydrophobicity of the the chain is increased or equivalently as ϵ_b is decreased the chain responds differently to TMAO. effect of 1 M TMAO solution is thus very sensitive to the value of ϵ_b . We find that the protecting role of TMAO is very weak when the chain is strongly hydrophobic (low values of $\epsilon_b = 0.4$ and 0.6 kJ/mol), in agreement with the conclusions of the previous study.²² However TMAO's protecting role becomes much more prominent for

larger values $\epsilon_b = 0.8$ and 1.0 kJ/mol.

As previously suggested using a different water model²⁹, the response of the polymer to urea on decreasing ϵ_b is radically different. The trend is clearly opposite to that found in water or in TMAO solution: the unfolded state gets stabilized while the collapsed state population progressively disappears, and a significant fraction of the population is found in the hairpin state. Urea therefore exhibits a typical denaturing effect. In strong contrast with TMAO and in agreement with a previous study²⁹, we show in the Figure 6 that urea readily denatures hydrophobic polymers (e.g. $\epsilon_b = 0.4$ kJ/mol) yet its denaturing effect becomes more prominent as ϵ_b increases.

To assess the robustness of our results, we also repeated our simulations $\epsilon_b = 1.0$ kJ/mol using a different water model³⁸ and found very similar results (see Appendix and Figure 8). Although the force-field we have employed for TMAO has been widely employed in the past and clearly behaves as a protective osmolyte,^{23,24,28} it has recently been criticized because it underestimates osmotic pressure at high solute concentrations.²⁶ We have repeated our simulations at 1 M using Garcia et al’s modified “osmotic”) version of this force-field.²⁶ As shown in Figure 7, its effect on the polymer chain nonetheless differs very little from what we observed using the aforementioned forcefield.

Our simulations show that TMAO acts as a protective osmolyte and urea as a denaturant on the polymer chain for $\epsilon_b = 1.0$ kJ/mol. TMAO thus acts on this chain similarly to the way it acts on many proteins as found experimentally⁶, showing that its effect extends to purely uncharged polymer chains of moderate hydrophobicity. TMAO’s ability to act as a protecting osmolyte depends on the properties of the polymer it is acting on as is shown by its sensitivity to the value of the polymer-bead ϵ_b : TMAO seems to have little effect on strongly hydrophobic chains. Urea, on the other hand still denatures them. In the following, we aim to better understand the effect of both osmolytes on the polymer chain with $\epsilon_b = 1.0$ kJ/mol.

B. Molecular Mechanism of Osmolyte-induced (un)folding

1. Interpretation based on preferential binding and chemical potential of osmolytes

It has been suggested in the literature that denaturants exhibit preferential interaction with protein surfaces while protective osmolytes are preferentially excluded from the surface⁴⁻⁸ because of unfavorable interactions^{6,8}. Therefore such behavior should be observed in both the local-bulk partition coefficient K_p (Eq. 1) and the preferential binding coefficient Γ (Eq. 2).

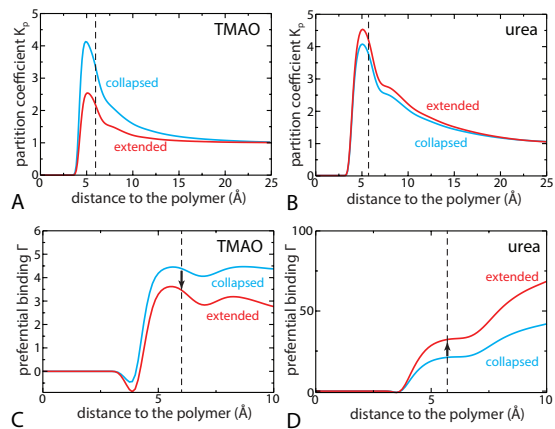


FIG. 4. Preferential binding constants of TMAO in 1 M TMAO (red) and urea in 7 M urea (green) as a function to the distance to the polymer (for chains with $\epsilon_b = 1.0$ kJ/mol), frozen in an collapsed (black) or extended (red) configurations extended configuration. Vertical dashed lines indicate the position of the polymer first solvation shell in each case (6 \AA for TMAO and 5.7 \AA for urea), and the black arrows in C and D represent the relevant value of $\Delta\Gamma$.

In Figure 4A-B we compare the dependence of K_p on polymer conformation as a function of distance from polymer in both TMAO and urea solutions. If the local domain is defined as the polymer’s first solvation shell, then the representatives values for K_p (and later Γ) should be taken near $\approx 6 \text{ \AA}$ (dashed line), which cor-

responds to the the first minima of the radial distribution functions between the polymer and cosolvent molecules (urea or TMAO). As expected, urea molecules accumulate next to both collapsed and extended states of the polymer, leading to $K_p > 1$ (Figure 4B). K_p is little sensitive to the polymer conformation but it is always slightly higher in the extended state. The local-bulk partition coefficient of TMAO is also *greater* than 1 (Figure 4A), implying that TMAO also *binds* to the polymer surface. This result contradicts the popular view that protective osmolytes are believed to be preferentially excluded from the protein surface⁴⁻⁸. However, this should not be surprising since TMAO is mostly hydrophobic and thus might be better accommodated in the polymer hydration shell than in bulk solution. But a key observation is that K_p displays significant conformation-dependence: it is higher near a collapsed configuration than near an extended configuration. Therefore, TMAO strongly interacts with the polymer ($K_p > 1$) but there is an effective depletion next to extended conformations of polymer relative to collapsed conformations.

Although the local-bulk partition coefficient provides a better description of the preferential interaction because of its intensive nature, it is not directly connected to experimental observables. In contrast, the preferential binding coefficient Γ can be measured experimentally, e.g. using the vapor-pressure osmometry technique⁷. The effect of preferential binding on a conformational equilibrium between the folded and the unfolded configurations $F \rightleftharpoons U$ (with an equilibrium constant K) is usually understood in terms of the thermodynamic calculation first introduced by Wyman and Tanford^{2,3}, which leads to

$$\frac{\partial \ln K}{\partial \ln a_s} = \Delta\Gamma_{F \rightarrow U}, \quad (4)$$

where a_s is the activity of the cosolvent in the binary solution. According to Eq. 4, an increase in the concentration of the cosolvent would lead to the biomolecule unfolding if $\Delta\Gamma > 0$, and in contrast would favor the folded state over the unfolded one if $\Delta\Gamma < 0$.

In Figure 4C-D we show the average preferential binding coefficients Γ for both collapsed and extended conformations in TMAO and urea solutions. As already discussed above, one should consider the Γ values at the distance corresponding to the polymer first solvation shell. Not surprisingly, in all cases Γ is positive, which is equivalent to $K_p > 1$ (Figure 4A-B). Similarly, the trends in the difference between the extended and collapsed configurations $\Delta\Gamma$ follow that of ΔK_p : $\Delta\Gamma$ is negative for TMAO, which stabilizes the folded state over the unfolded one, while the positive $\Delta\Gamma$ for urea clearly corresponds to its denaturing effect. Our results are therefore in agreement with the current consensus on the osmolyte effect⁴⁻⁸ summarized by Eq.4.

The main difference between our work and previous studies on proteins is that the sign of $\Delta\Gamma$ is different from that of Γ for TMAO (they have the same sign for urea). This surprising observation can be understood if we consider the relationship between K_p and Γ . Indeed combining Eqs. 1 and 2 with the hypothesis that the bulk domain is large with respect to the local domain (i.e., $\langle n_X \rangle \ll N_X^{tot}$), leads to

$$\Gamma = \langle n_s \rangle \left(1 - \frac{1}{K_p} \right). \quad (5)$$

Therefore $\Delta\Gamma$ will depend on both $\Delta\langle n_s \rangle$ and $\Delta(1/K_p)$ (note that these two terms are not independent of each other). In experimental studies of proteins, it was found that Γ is proportional to the solvent surface accessible area S^7 . Since $\langle n_s \rangle$ is also proportional to S , K_p is expected to be the same whether the protein is folded or not. This may not be surprising given that the nature of the exposed groups is the same in the folded and the unfolded state. However for our polymer, K_p is very much conformation-dependent, while n_s is only marginally higher in the extended state. This therefore provides an explanation for why $\Delta\Gamma$ is negative while TMAO always accumulates in the hydration shell ($\Gamma > 0$). Finally, it is interesting to note that simulations of decaalanine have found Γ to be positive for TMAO²⁸ even though it was observed to behave as a pro-

tective osmolyte.

2. *Conformation-dependence of the osmolyte chemical potentials in the polymer first solvation shell*

To obtain a better understanding of how TMAO can preferentially bind to the polymer surface, yet still behave as a protective osmolyte favoring the polymer collapsed state, we investigate the free-energy changes (chemical potential) associated with the insertion of a single osmolyte or water molecule next to different conformations (both collapsed and extended) of the polymer. These chemical potentials were determined from thermodynamic integration (see Methods, Appendix and Figures 9 and 10). Insertion of a TMAO and a water molecule in the 1 M TMAO solution (or urea and water in the 7 M urea solution) was considered in three different cases: in the bulk, i.e. far from the polymer; in the first hydration shell of the polymer frozen in a *collapsed* configuration; and in the first hydration shell of polymer frozen in an *extended* configuration.

Table I lists the results of thermodynamic integration; namely, the van der Waals and electrostatic contributions to the chemical potentials of urea and TMAO in the different cases. In all cases insertion of a osmolyte molecule is more favorable next to the polymer than it is in the bulk: this is in agreement with the preferential binding values discussed above. However, the chemical potentials of TMAO and urea, relative to bulk values follow opposite trends as far as the conformation-dependence is concerned. An inserted single TMAO molecule is more stable (has lower free energy) next to the *collapsed* conformation of polymer than next to the *extended*. Its free-energy is lower by 0.8 kcal/mol per TMAO molecule. This is mainly due to the more favorable free energy contribution from the van der Waals interaction, which overcomes the slight destabilization in the electrostatic contribution in the collapsed conformation due to less exposure to water or other TMAO molecules in the collapsed state

than in the extended state. Given the importance of the van der Waals term for this (mostly) hydrophobic molecule, the total free-energy change is dominated by this contribution. In urea, however, the van der Waals term is small and does not totally compensate the electrostatic contribution. Therefore the insertion of a urea molecule is more favorable next to the extended state.

The observed differences and respective contributions of van der Waals and electrostatic free-energy, which drive the preferential interaction with one state or another, suggest a mostly enthalpic origin to this behavior. This is confirmed by considering the distributions of both van der Waals and electrostatic energy distributions for single osmolyte molecule in the hydration shell of the polymer, either in a collapsed or in an extended conformation (see Appendix and Table III). The observed trends are similar to that found from the FEP study — TMAO interacts preferentially with the polymer collapsed state because of the van der Waals contribution, leading to a difference of ≈ 0.2 kcal/mol as compared to the extended state and ≈ 0.5 kcal/mol with respect to the bulk phase. In contrast, a slight stabilization of urea in the extended polymer hydration shell with respect to the collapsed state is found (≈ 0.2 kcal/mol) and appears to be driven by the electrostatic contribution. In both cases, a significant stabilization is found as compared to the bulk phase (≈ 1.5 kcal/mol).

3. *A free-energy based model for action of protecting and denaturing osmolyte*

The discussion in the previous paragraphs have focussed on only the contributions of the chemical potential of osmolyte (TMAO or urea) to the free-energy difference between the polymer collapsed and the extended states. We now try to build a free energy-based thermodynamic model based on the above FEP data, with the goal of validating it against the net PMF profiles of the polymer in the respective solutions (as previously discussed in Figure 3). The net

System	G_{vdw}	$G_{coulomb}$	G_{total}	$\Delta\mu^{bulk}$	$\langle N_k \rangle$
TMAO					
bulk	+1.99(0.02)	-13.97(0.02)	-11.97(0.01)	0	-
collapsed	-0.52(0.36)	-13.08(0.22)	-13.60(0.27)	-1.63	6.2(0.2)
extended	+1.04(0.45)	-13.80(0.08)	-12.76(0.38)	-0.79	6.3(0.6)
urea					
bulk	-0.17(0.04)	-13.27(0.05)	-13.44(0.09)	0	-
collapsed	-1.33(0.71)	-12.45(0.53)	-13.78(0.20)	-0.33	28.6(0.3)
extended	-0.99(0.29)	-12.91(0.23)	-13.90(0.15)	-0.46	41.9(0.8)

TABLE I. Different free-energy contributions (in units of kcal/mol) for inserting single osmolyte molecules in the first solvation shell of the polymer (with $\epsilon_b = 1.0$ kJ/mol) in 1 M TMAO and 7 M urea. $\Delta\mu^{bulk}$ represents the difference with respect to the bulk solution, and the average number of molecules in first solvation shell of the polymer N_k is also given. Standard deviations are given within parentheses.

free-energy change for going from a collapsed to an extended configuration can be expressed as

$$\begin{aligned}
\Delta G^{C-E} &= \Delta G_{gas}^{C-E} + \sum \Delta G_k^{C-E} \\
&= \Delta G_{gas}^{C-E} + \Delta G_w^{C-E} + \Delta G_{cs}^{C-E} \\
&= \Delta G_{gas}^{C-E} + [N_w^E \mu_w^E - N_w^C \mu_w^C] \\
&\quad + [N_s^E \mu_s^E - N_s^C \mu_s^C] \quad (6)
\end{aligned}$$

where N_k^C (respectively N_k^E) is the average number of solvent molecules of type k (water w or osmolyte s) in the first hydration shell of the polymer in a collapsed (respect. extended) configuration, and μ_k^C (respect. μ_k^E) their associated chemical potentials. We assume here that the chemical potentials of molecules beyond the first hydration shell are similar for both polymer configurations.

To evaluate Eq. 6, we must separately determine three individual contributions:

(a) The first term of the equation corresponds to the free-energy difference between the collapsed and extended states of the polymer itself in gas phase. It was obtained by repeating our simulations in the gas phase and by performing umbrella sampling calculations to estimate the free-energy difference between the collapsed and the extended state in the absence of solvent, which was found to be $\Delta G_{gas}^{C-E} = 9.6$ kcal/mol in favor of the *collapsed* conformation.

(b) To calculate the second term, which describes water's contribution to the total free energy difference, we repeated our FEP calculations for water as well using the same method as detailed above for the osmolyte molecules. Results are reported in Table II. In all cases (bulk, TMAO or urea solutions), the difference in chemical potential between inserting a water molecule next to the collapsed or next to the extended state is very small, and slightly negative with respect to bulk. At the same time, the hydration number is significantly increasing because of a larger surface area in the extended state. Both the changes in chemical potential $\delta\mu_w = \mu_w^E - \mu_w^C$ and that of the number of molecules $\delta N_w = N_w^E - N_w^C$ contribute to the total free-energy difference between the collapsed and the extended state due to water molecules. A detailed analysis discussed in the Appendix and Table IV shows that in all cases, the dominant contributions logically arise from δN_w .

(c) The third term describes contribution of osmolyte molecules (TMAO or urea) to the net free energy difference. The chemical potentials in each configuration were already discussed and are given in Table I, which also contains the total number of osmolyte molecules in the polymer first hydration shell. Similarly to water, we

System	$\Delta\mu^{bulk}$	$\langle N_k \rangle$
pure water	collapsed -0.17(0.04)	73.8
	extended -0.15(0.02)	111.3
TMAO	collapsed -0.08(0.05)	66.9
	extended -0.11(0.04)	106.6
urea	collapsed -0.13(0.14)	33.0
	extended -0.17(0.31)	43.5

TABLE II. Total free-energy cost $\Delta\mu^{bulk}$ (with respect to the bulk solution reference) for inserting single water molecules in the first solvation shell of the polymer (with $\epsilon_b = 1.0$ kJ/mol) in pure water, 1 M TMAO and 7 M urea (in units of kcal/mol), and average number of water molecules in the polymer first hydration shell N_k . Standard deviations are given within parentheses.

can define $\delta\mu_s = \mu_s^E - \mu_s^C$ and $\delta N_s = N_s^E - N_s^C$. For urea, both the $\delta\mu_s$ and δN_s bring a negative contribution to the solvent-induced free-energy difference, which therefore favors the extended state. For TMAO, the two terms bring opposite contributions (Appendix and Table IV). While $\delta N_s > 0$ favors the extended conformation, it is the dominant contribution of the large $\delta\mu_s$ that leads to a positive ΔG_s^{C-E} , stabilizing the collapsed state relative to the extended one.

Figure 5 represents these three different individual contributions schematically. In pure water, the water contribution favors the *extended* state, as shown above. However, it does not totally compensate the polymer contribution (this will depend on the value of ϵ), so that the folded state is still the most stable in this case, as calculated independently with our umbrella sampling simulations (Figure 3). In the TMAO solution, the water contribution is only slightly perturbed with respect to the pure water case, but TMAO molecules will bring a contribution favoring the *collapsed* state, in agreement with our earlier estimation based on PMF

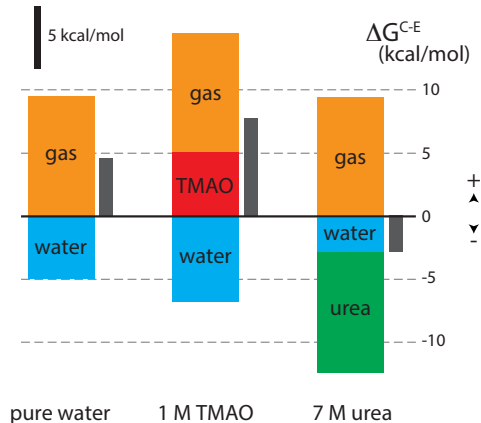


FIG. 5. Histograms showing the different contributions to the free-energy cost of inserting water or osmolyte molecules in the polymer hydration shell.

calculations (Figure 3). Finally in the urea solution, the urea contribution stabilizes the *extended* conformation greatly so that the overall free-energy difference becomes favorable towards extended conformations, as we have observed.

The semi-quantitative agreement that is observed in all three cases with the free-energy differences calculated from umbrella sampling simulations further validates the current approach. Note however that for TMAO and urea solutions, we systematically overestimate the respective stabilization. A possible explanation for this discrepancy is that we consider only a few sites for insertion of an osmolyte or a water molecule in the hydration shell. However, the fact that the trend is correctly and self-consistently predicted and also that the energy distributions exhibit exactly the same behavior makes us confident in this approach. Finally, the decomposition presented in the Appendix in terms of the respective contributions of $\delta\mu_s$ and δN_s also suggests that an osmolyte's behavior cannot be predicted from the sign of $\delta\mu_s$ alone, as detailed in the Appendix.³⁹

IV. CONCLUSIONS

In this paper, we considered the effect of osmolytes (TMAO and urea) on a simple polymer, consisting of a short Lennard-Jones chain similar to an alkane or lipid chain in aqueous solutions of the two osmolytes. This model is reminiscent of the model used in our previous paper²⁹ directed at understanding urea denaturation of hydrophobic collapse.

Here we determined the free energy landscapes of the hydrophobic polymer as a function of its radius of gyration. We show that 1 M TMAO and 7 M urea act dramatically differently on model polymer chains and their behaviors are sensitive to the strength of the attractive dispersion interactions of the chain with its environment: when these dispersion interactions are high enough, TMAO suppresses the formation of extended conformations of the hydrophobic polymer as compared to water, while urea promotes formation of extended conformations. Quite surprisingly, we find that *both* protecting and denaturing osmolytes strongly interact with the polymer (with both having a preferential binding constant greater than zero), in contrast with existing explanations of the osmolyte effect. An extensive free energy analysis suggests that protective osmolytes are *not* necessarily excluded from the polymer surface. What really matters is the *effective depletion* of the osmolyte as the polymer conformation changes, in agreement with the current consensus on the osmolyte effect⁴⁻⁸. Indeed for TMAO, it is the much more favorable free energy of insertion of a single osmolyte near the collapsed configurations of the polymer than near the extended configurations that dictates its propensity to drive the system towards the collapsed conformation, and therefore to lead to its protective effect. This appears to be driven by van der Waals interactions. In contrast, urea is preferentially stabilized next to the extended conformation because the smaller van der Waals contributions do not compensate the electrostatic contribution, suggesting this as an explanation of its denaturing effect.

A thermodynamic model taking into account

the different contributions (gas-phase, water and osmolyte) to the polymer conformational equilibrium was developed. In the aqueous solution of urea, the free energy contribution coming from urea and water easily cooperates to shift the polymer towards extended conformations of the polymer. In the aqueous solution of TMAO, TMAO's free energy contribution favors the collapsed conformation and it is able to overcome the water's free energy contribution which favors the extended conformation: overall, the equilibrium is shifted towards the collapsed conformation.

We believe that this simple thermodynamic model provides an interesting perspective for explaining the role of protecting and denaturing osmolytes on simple macromolecules. Although the model is very simple, it provides fresh insights on the action of various osmolytes. Manipulation of simple polymers at the single molecule level has been recently achieved⁴⁰ and we believe that the effect of osmolytes such as urea or TMAO on the polymer conformational equilibrium could be probed by such techniques. From a simulation perspective, it will be interesting in the future to extend our free-energy based approach to systems of increasing complexity like charged polymers, real peptides or proteins to shed light on the role of osmolytes on macromolecular conformations.

V. ACKNOWLEDGMENTS

This work was supported by grants from the National Institutes of Health [NIH-GM4330 (to B.J.B.)] and by the National Science Foundation through [via Grant No. NSF-CHE-0910943]. We gratefully acknowledge the computational support of the Computational Center for Nanotechnology Innovations (CCNI) at Rensselaer Polytechnic Institute (RPI). This work used the Extreme Science and Engineering Discovery Environment (XSEDE), which is supported by National Science Foundation grant number OCI-1053575.

Appendix A: Effect of the polymer bead parameter ϵ_b on the polymer conformational equilibrium

To investigate how variations of the polymer bead parameter ϵ_b affect its behavior in the various solutions we repeated our simulations using 3 other values of ϵ_b (0.4, 0.6 and 0.8 kJ/mol). Note that the lower the value of this energy parameter the more hydrophobic is the chain. Results are presented in Figure 6.

In pure water the unfolded state gets stabilized relative to the collapsed state as ϵ_b decreases (that is $\Delta G_{F \rightarrow U}$ gets less positive) as ϵ_b decreases. When changing the ϵ_b parameter, there is a competition between two opposite effects: first, as ϵ_b decreases this will decrease the interaction between beads and water molecules, thereby increasing the hydrophobic character of the chain and driving the polymer towards toward collapsed configurations. However at the same time, the intramolecular interactions will decrease, which would favor more extended states. Our results suggest that this later contribution dominates. In 1 M TMAO solution we observe that the protective effect is very sensitive to variations in ϵ_b : indeed the protecting role evidenced above at $\epsilon_b = 1$ kJ/mol is moderate to almost nonexistent when the chain is really hydrophobic (low values of $\epsilon_b = 0.4$ and 0.6 kJ/mol), in agreement with a previous study²²: the osmolyte effect becomes more prominent only for $\epsilon_b = 0.8$ and 1.0 kJ/mol. In strong contrast with TMAO and in agreement with a previous study²⁹, urea still readily denatures hydrophobic polymers at small $\epsilon_b = 0.4$ kJ/mol) yet its denaturing effect becomes more prominent as ϵ_b increases.

Appendix B: Effect of a different forcefield for TMAO on the free energy profile

The force-field we have employed throughout our entire study for TMAO (known as 'Kast model')³² has also been recently modified by Garcia and coworkers²⁶ and a new forcefield, termed the 'osmotic model' has also been pro-

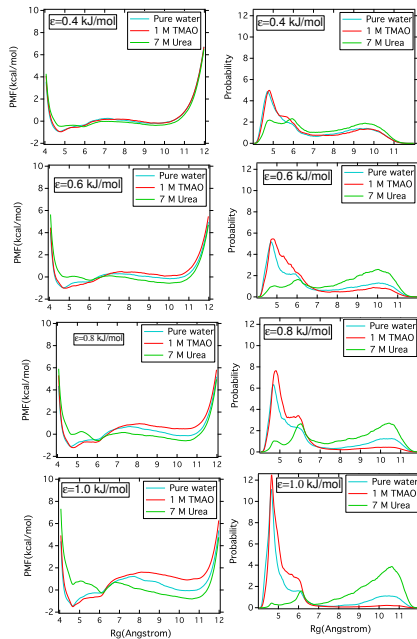


FIG. 6. PMFs along the radius of gyration (left) and the corresponding probability distributions (right) for four different polymer dispersion interactions ($\epsilon = 0.4$ kJ/mol, 0.6 kJ/mol, 0.8 kJ/mol and 1.0 kJ/mol) in three aqueous solutions (water, blue; TMAO, red and urea, green). The PMFs $W(R_g)$ are normalized so that $\int_0^\infty \exp(-W(r)/k_B T) dr = 1$

posed by them. We repeated our umbrella sampling simulations for free energy profile at 1 M using this modified version of this force-field. As shown in the Figure 7, its effect on the polymer chain is similar to that obtained from the original 'Kast model' of TMAO .

Appendix C: Effect of a different water model on the free energy profile

All the results reported in the main article were obtained using the SPC/E water model³⁰. However, for the purpose of testing the robustness of our results with respect to the different water models, we have repeated our computation of free energy profiles using a different water model, namely TIP4P water³⁸, mainly

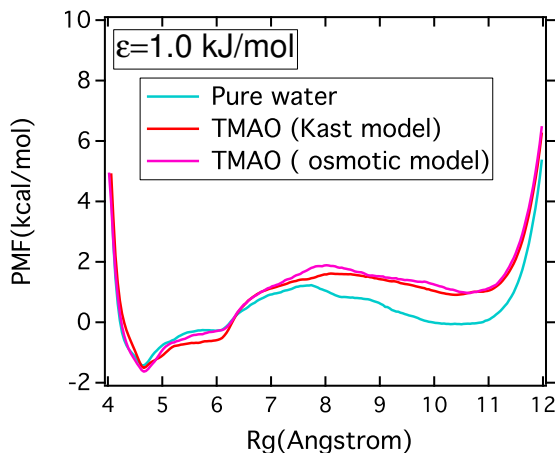


FIG. 7. Effect of different TMAO forcefields on free energy profile of polymeric chain in 1 M TMAO. ‘Osmotic model’ is the modified version of TMAO forcefield as proposed by Garcia and co-workers and ‘Kast model’ is the original TMAO forcefield (used in the rest of the current study). We also show the free energy profile of the polymeric chain in pure water.

because it was used in our previous work on urea²⁹. Figure 8 compares the effect of the two different water models on the free energy profiles of the polymeric chain ($\epsilon_b = 1.0$ kJ/mol) in different osmolyte solutions. The common trend prevalent in all free energy profiles corresponding to TIP4P water model is that the free energy barrier $\Delta G_{F \rightarrow U}^\ddagger$ for the transformation from the compact to the extended state in pure water and in 1 M TMAO are respectively higher for TIP4P water than for SPC/E water. For 7 M urea, the extent of free energy of stabilization is negligibly more favorable in SPC/E water than in TIP4P water. But, interestingly, the relative free energy difference $\Delta\Delta G_{F \rightarrow U}$ of the chain in going from pure water to 1 M TMAO solution or 7 M urea solution is almost the same for both SPC/E and TIP4P water models.

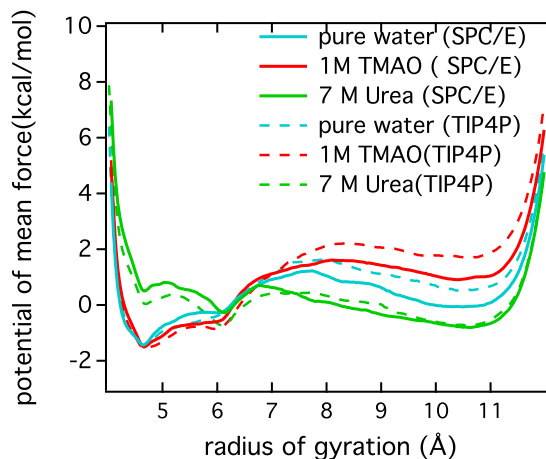


FIG. 8. Comparison of different free energy profiles of polymeric chain ($\epsilon_b = 1.0$ kJ/mol) obtained using SPC/E water model (solid lines) with that obtained from TIP4P water model (dashed lines).

Appendix D: Thermodynamic integration

As detailed in the Methods section, we performed free-energy perturbation calculations to estimate the cost of inserting water or cosolvent molecules at different positions in the polymer hydration shell, or in the bulk. The interactions of the molecule being inserted were slowly turned on in two stages: in the first stage only the van der Waals interactions were turned on, and in the second stage the electrostatic interactions were turned on. Thermodynamic integration thus yields two contributions to the transfer free energy. In Figure 9, we present results of thermodynamic integration for the two stages and compare insertion of a single TMAO at a given position in the bulk, in the hydration shell of the polymer in a collapsed configuration, and in the hydration shell of the polymer in an extended configuration. The thermodynamic data confirms that van der Waals contribution to the free energy of inserting a single TMAO is more favorable near a collapsed conformation than near an extended conformation, and it more than compensates the favorable electrostatic contribution near an extended

conformation than that near the collapsed conformation. In Figure 10, we present the same data for inserting a single urea molecule in the urea solution, where the reverse trend is observed: the more favorable electrostatic contribution to the free energy of inserting a single urea near the extended conformation overcomes the favorable van der Waals contribution to free energy of inserting a single urea near the collapsed conformation.

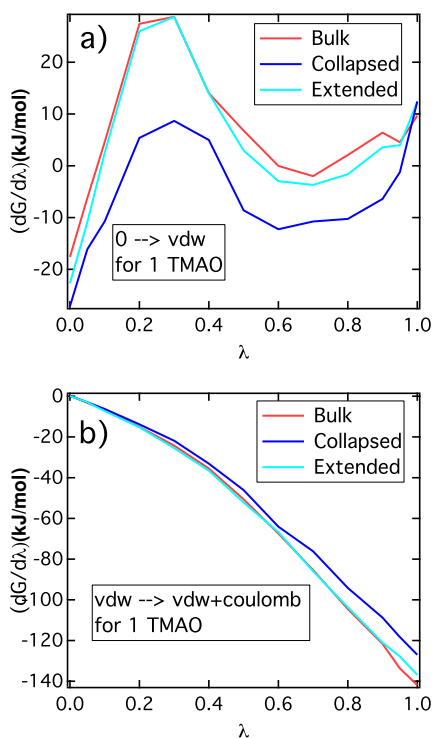


FIG. 9. Comparison of thermodynamic integration profile of turning on a) the van der Waals interactions and then b) the electrostatic interaction of a single TMAO molecule near the polymer for different polymer conformations in 1 M TMAO solution.

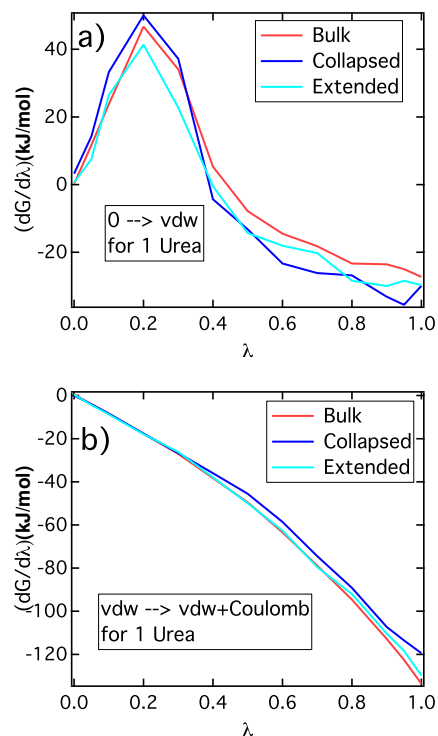


FIG. 10. Comparison of thermodynamic integration profile of turning on a) the van der Waals interactions and b) the electrostatic interactions of a single urea molecule near the polymer for different polymer conformations in 7 M urea solutions.

Appendix E: Energy distribution in the polymer first hydration shell

Table III provides details on the respective net average energies and the individual van der Waals and electrostatic contributions to these energies for a single cosolute molecules (TMAO and urea). The observed trends in the average energy analysis are consistent with that found from the FEP study — TMAO interacts preferentially with the polymer collapsed state because of the favorable LJ contribution. In contrast, a slight stabilization of urea in the extended polymer hydration shell with respect to the collapsed state is found to be driven by the electrostatic contribution.

System	E_{vdw}	$E_{coulomb}$	E_{total}	ΔE^{bulk}
TMAO				
bulk	-3.824(2.22)	-29.510(4.71)	-33.334(3.82)	0
collapsed	-5.853(2.62)	-27.985(4.90)	-33.838(3.93)	-0.504
extended	-5.404(2.41)	-28.231(4.83)	-33.635(3.89)	-0.301
urea				
bulk	-5.079(2.55)	-28.234(5.16)	-33.313(4.21)	0
collapsed	-8.451(2.54)	-26.329(4.90)	-34.780(3.98)	-1.467
extended	-8.002(2.61)	-26.993(4.89)	-34.995(3.99)	-1.682

TABLE III. Different average energy contributions (in units of kcal/mol) of single cosolute molecules in the first solvation shell of the polymer in 1 M TMAO and 7 M urea. ΔE^{bulk} represents the difference with respect to the bulk solution. Standard deviations are given within parentheses.

Appendix F: Decomposition of the solvent contributions to polymer collapse

In the pure solvent as well as in a mixture of water and a cosolute (TMAO or urea), the contribution of the species k to the free-energy difference between the collapsed and the extended state can be expressed as

$$\Delta G_k^{C-E} = N_k^E \mu_k^E - N_k^C \mu_k^C \quad (\text{F1})$$

where N_k^C (respectively N_k^E) is the number of solvent molecules of type k in the first hydration shell of the polymer in a collapsed (respect. extended) configuration, and μ_k^C (respect. μ_k^E) their associated chemical potentials. We can define the relative changes for both quantities as $N_k^E = N_k^C + \delta N_k$ and $\mu_k^E = \mu_k^C + \delta \mu_k$. Substituting N_k^E and μ_k^E in Eq. F1 leads after simplification to

$$\Delta G_k^{C-E} = N_k^C \delta \mu_k + \mu_k^C \delta N_k + \delta N_k \delta \mu_k \quad (\text{F2})$$

The first term on the right hand side of Eq. F2 represents the contribution of the change in chemical potential, for a fixed number of molecules in the hydration shell; the second term represents the contribution of the change in the hydration number for a fixed chemical potential. The last one is a second-order term, whose contribution is expected to be minor.

Case	$N_k^C \delta \mu_k$	$\mu_k^C \delta N_k$	$\delta N_k \delta \mu_k$	ΔG_k^{C-E}
TMAO	+5.2	-0.2	+0.10	+5.1
urea	-3.5	-4.5	-1.6	-9.6
water (bulk)	+0.8	-6.2	+0.4	-5.0
water (TMAO)	-2.4	-3.1	-1.4	-6.9
water (urea)	-1.1	-1.4	-0.4	-2.9

TABLE IV. Different free-energy contributions (in units of kcal/mol) of Eq. F2

The different free-energy contributions for each solvent type is given in Table IV. In all cases, the chemical potential of a water or cosolute (TMAO and urea) molecule in the hydration shell is lower than in bulk, so that $\mu_k^C \delta N_k$ is negative. This represents the main contribution to the free-energy difference induced by water (in all solutions) and urea, showing that the large change in the hydration number is responsible for the increased solvent-induced stability of the unfolded state over the collapsed one. The situation is markedly different for TMAO. The large change in μ_s when going from collapsed to extended is bringing a large $\delta N_s \delta \mu_s$ contribution, which is positive and not totally compensated by the $\mu_s^C \delta N_s$ term (the

$\delta N_s \delta \mu_s$ term brings an additional positive contribution). Therefore the total free-energy difference is positive, in strong contrast with what is observed for urea and water.

The above decomposition also suggests that an osmolyte's behavior cannot be predicted from the sign of $\delta \mu_s$ alone. Indeed the main δN_s contribution (which is equal to $\mu_s^C \delta N_s$) can overcome that of $\delta \mu_s$ if the following criteria are met: (i) the stabilization in the polymer hydra-

tion shell with respect to the bulk is large, but the variation between the collapsed and the extended state is small ($\mu_s \ll 0$ and $\delta \mu_s \approx 0$); (ii) the osmolyte can accumulate in the hydration shell, i.e. δN_s is largely positive. In other words, this situation can arise if the relative variations of the hydration number when going from collapsed to extended conformations are larger than that of the associated chemical potentials, even if the cosolute molecules are more stable around the collapsed conformations.

* bb8@columbia.edu

- ¹ P. H. Yancey, M. E. Clark, S. C. Hand, R. D. Bowlus, and G. N. Somero, *Science* **217**, 1214 (1982).
- ² J. Wyman, *Adv. Protein Chem.* **19**, 223 (1964).
- ³ C. Tanford, *J. Mol. Biol.* **39**, 539 (1969).
- ⁴ S. N. Timasheff, *Proc. Natl. Acad. Sci. USA* **99**, 9721 (2002).
- ⁵ V. A. Parsegian, R. P. Rand, and D. C. Rau, *Proc. Natl. Acad. Sci. USA* **97**, 3987 (2000).
- ⁶ D. Bolen and G. Rose, *Annu. Rev. Biochem.* **77**, 339 (2008).
- ⁷ E. S. Courtenay, M. W. Capp, C. F. Anderson, and M. T. Record, Jr, *Biochemistry* **39**, 4455 (2000).
- ⁸ D. R. Canchi and A. E. García, *Annu. Rev. Phys. Chem.* **64**, 273 (2013).
- ⁹ T. O. Street, D. W. Bolen, and G. D. Rose, *Proc. Natl. Acad. Sci. USA* **103**, 13997 (2006).
- ¹⁰ A. J. Wang and D. W. Bolen, *Biochemistry* **36**, 9101 (1997).
- ¹¹ T. Y. Lin and S. N. Timasheff, *Biochemistry* **33**, 12695 (1994).
- ¹² J. Tatzelt, S. Prusiner, and W. Welch, *EMBO J.* **15**, 6363 (1996).
- ¹³ P. K. Nandi, A. Bera, and P.-Y. Sizaret, *J. Mol. Biol.* **362**, 810 (2006).
- ¹⁴ H. C. Tseng and D. J. Graves, *Biochem. Biophys. Res. Comm.* **250**, 726 (1998).
- ¹⁵ F. Scaramozzino, D. W. Peterson, P. Farmer, J. T. Gerig, D. J. Graves, and J. Lew, *Biochemistry* **45**, 3684 (2006).
- ¹⁶ V. N. Uversky, J. Li, and A. L. Fink, *FEBS Lett.* **509**, 31 (2001).
- ¹⁷ J. P. Morello, U. E. Petaja-Repo, D. G. Bichet, and M. Bouvier, *Trends Pharmacol. Sci.* **21**, 466 (2000).
- ¹⁸ W. H. W. Tang, Z. Wang, B. S. Levison, R. A. Koeth, E. B. Britt, X. Fu, Y. Wu, and S. L. Hazen, *N. Engl. J. Med.* **368**, 1575 (2013).
- ¹⁹ B. J. Bennion and V. Daggett, *Proc. Natl. Acad. Sci. USA* **101**, 6433 (2004).
- ²⁰ K. A. Sharp, B. Madan, E. Manas, and J. M. Vanderkooi, *J. Chem. Phys.* **114**, 1791 (2001).
- ²¹ J. Hunger, K.-J. Tielrooij, R. Buchner, M. Bonn, and H. J. Bakker, *J. Phys. Chem. B* **116**, 4783 (2012).
- ²² M. V. Athawale, J. S. Dordick, and S. Garde, *Biophys. J.* **89**, 858 (2005).
- ²³ S. S. Cho, G. Reddy, J. E. Straub, and D. Thirumalai, *J. Phys. Chem. B* **115**, 13401 (2011).
- ²⁴ C. Y. Hu, G. C. Lynch, H. Kokubo, and B. M. Pettitt, *Proteins* **78**, 695 (2010).
- ²⁵ G. Stirnemann, J. T. Hynes, and D. Laage, *J. Phys. Chem. B* **114**, 3052 (2010).
- ²⁶ D. R. Canchi, P. Jayasimha, D. C. Rau, G. I. Makhatadze, and A. E. Garcia, *J. Phys. Chem. B* **116**, 12095 (2012).
- ²⁷ S. Paul and G. N. Patey, *J. Phys. Chem. B* **111**, 7932 (2007).
- ²⁸ H. Kokubo, C. Hu, and B. M. Pettitt, *J. Am. Chem. Soc.* **133**, 1849 (2011).
- ²⁹ R. Zangi, R. Zhou, and B. J. Berne, *J. Am. Chem. Soc.* **131**, 1535 (2009).
- ³⁰ H. J. C. Berendsen, J. R. Grigera, and T. P. Straatsma, *J. Phys. Chem.* **91**, 6269 (1987).
- ³¹ E. M. Duffy, D. Severance, and W. L. Jorgensen, *Isr. J. Chem.* **33**, 323 (1993).
- ³² K. M. Kast, J. Brickman, S. M. Kast, and R. S. Berry, *J. Phys. Chem. A* **107**, 5342 (2003).
- ³³ B. Hess, C. Kutzner, D. Van der Spoel, and E. Lindahl, *J. Chem. Theory Comput.* **4**, 435 (2004).

- (2008).
- ³⁴ M. Bonomi, D. Branduardi, G. Bussi, C. Camilloni, and M. Parrinello, *Comp. Phys. Comm.* **180**, 1961 (2009).
- ³⁵ S. Kumar, D. Bouzida, R. H. Swendsen, P. A. Kollman, and J. M. Rosenberg, *J. Comput. Chem.* **13**, 1011 (1992).
- ³⁶ A. Grossfield, “Wham: the weighted histogram analysis method, version 2.0,” <http://membrane.urmc.rochester.edu/content/wham>.
- ³⁷ D. Shukla, C. Shinde, and B. L. Trout, *J. Phys. Chem. B* **113**, 12546 (2009).
- ³⁸ W. Jorgensen, J. Chandrasekhar, J. Madura, R. Impey, and M. Klein, *J. Chem. Phys.* **79**, 926 (1983).
- ³⁹ Indeed the main δN_s contribution (which is equal to $\mu_s^C \delta N_s$) can overcome that of $\delta \mu_s$ if the relative variations of the hydration number when going from collapsed to extended conformations are larger than that of the associated chemical potentials, even if the osmolyte molecules are more stable around the collapsed conformations.
- ⁴⁰ I. T. S. Li and G. C. Walker, *Proc. Natl. Acad. Sci. USA* **108**, 16527 (2011).